Extreme-Mass-Ratio Inspirals Embedded in Dark Matter Halo: Chaotic Imprints in Gravitational Waves

Surojit Dalui
In collaboration with Surajit Das, Yi-Fu Cai and Bum-Hoon Lee
arXiv:2511.03657, 2512.04848

Shanghai University

SASGAC 2025

Outline

GW Astronomy in Two Bands

- Ground-based (Hz–kHz): LIGO/Virgo/KAGRA $\Rightarrow$ stellar-mass mergers.
- Space-based (mHz): LISA / TianQin / Taiji $\Rightarrow$ EMRIs, massive BH binaries, DWDs.
- **Open question:** do near-horizon nonlinearities (chaos) leave robust imprints in EMRI waveforms?

Why EMRIs? Why Chaos?

- EMRI: compact secondary ($m \ll M$) orbits MBH for $\sim 10^5$–10^6 cycles $\Rightarrow$ high-fidelity probe of strong gravity.
- Non-integrabilities near horizon (with environment) $\Rightarrow$ onset of chaos, broken KAM tori.
- **Goal:** connect phase-space chaos $\leftrightarrow$ observable GW signatures.

Astrophysical Motivation: Dark Matter Halos

- SMBHs live in galaxies embedded in DM halos.
- DM modifies spacetime in the nuclear region (effective metric corrections).
- We model a Schwarzschild-like BH *immersed* in a Dehnen $(\alpha, \beta, \gamma) = (1, 4, 5/2)$ halo; study test-particle chaos and its GW imprint.

Dehnen Density Profile

$$\rho(r) = \rho_s \left(\frac{r}{r_s}\right)^{-\gamma} \left[\left(\frac{r}{r_s}\right)^{\alpha} + 1\right]^{\frac{\gamma-\beta}{\alpha}}, \quad (\alpha, \beta, \gamma) = (1, 4, 5/2).$$

- ρ_s: characteristic density; r_s: scale radius.
- Cumulative mass: $M_{\rm DM}(r) = 4\pi \int_0^r \rho(x)\, x^2\, dx$.

From Tangential Velocity to Redshift Function

Consider the DM-dominated SSS metric

$$ds^2 = -A(r)dt^2 + \frac{dr^2}{B(r)} + r^2 d\Omega^2.$$

For circular orbits in a static geometry,

$$v_D^2 = r\,\frac{\mathrm{d}}{\mathrm{d}r}\big(\ln\sqrt{A}\big) = \frac{rA'(r)}{2A(r)}.$$

For Dehnen $(1, 4, 5/2)$ one finds

$$v_D^2(r) = \frac{M_{\rm DM}(r)}{r} = \frac{8\pi\rho_s r_s^3}{r}\sqrt{1+\frac{r_s}{r}}.$$

Integration

Integrate $\dfrac{A'}{A} = \dfrac{2v_D^2}{r}$ to obtain $A(r)$.

Redshift Function and Leading-Order Approximation

$$A(r) = \exp\left[-32\pi\rho_s r_s^2 \sqrt{\frac{r+r_s}{r}}\right],$$

$$A(r) \approx 1 - 32\pi\rho_s r_s^2 \sqrt{\frac{r+r_s}{r}} \quad \text{(leading order)}.$$

- We adopt the simplifying and accurate SSS ansatz $A(r) = B(r)$.
- Embed a Schwarzschild BH as a correction on top of the halo metric.

Combined BH+DM Spacetime

$$ds^2 = -f(r)\,dt^2 + \frac{dr^2}{f(r)} + r^2 d\Omega^2,$$

$$f(r) = 1 - \frac{2M}{r} - 32\pi\rho_s r_s^2 \sqrt{\frac{r + r_s}{r}}\,.$$

- Reduces to Schwarzschild for $\rho_s = 0$ or $r_s = 0$.
- DM terms increase effective horizon size.

Painlevé–Gullstrand (PG) Coordinates

Time transform: $dt \to dt - \dfrac{\sqrt{1-f(r)}}{f(r)}\,dr$.

$$ds^2 = -f(r)\,dt^2 + 2\sqrt{1-f(r)}\,dt\,dr + dr^2 + r^2 d\Omega^2.$$

- Regular across r_{H}; robust for near-horizon numerics.

Constants of Motion and Dispersion

In PG coordinates, with canonical momenta p_μ:

$$g^{\mu\nu} p_\mu p_\nu = -m^2, \qquad E = -\zeta^{(t)} \cdot p, \quad L = \zeta^{(\varphi)} \cdot p.$$

For motion in meridional plane $\{r, \phi\}$,

$$E = -\sqrt{1 - f(r)}\, p_r + \sqrt{p_r^2 + \frac{p_\phi^2}{r^2} + m^2}\,.$$

Confining Potentials and Physical Rationale

- Add integrable harmonic potentials to prevent plunge/escape:

$$V_{\text{ext}} = \tfrac{1}{2} K_r (r - r_c)^2 + \tfrac{1}{2} K_\phi \, r_{\text{H}}^2 (\phi - \phi_c)^2.$$

- Chaos originates from near-horizon unstable structure (inverted-oscillator-like peak in effective potential), not from the harmonic terms.
- Enables long, controlled near-horizon evolution to probe onset-of-chaos.

Total Energy with Confinement

$$E(r,\theta,p_r,p_\phi) = -\sqrt{1-f(r)}\,p_r + \sqrt{p_r^2 + \frac{p_\phi^2}{r^2} + m^2} + \frac{K_r}{2}(r-r_c)^2 + \frac{K_\phi}{2}\,r_{\mathrm{H}}^2(\phi-\phi_c)^2.$$

Equations of Motion

$$\dot{r} = \frac{\partial E}{\partial p_r} = -\sqrt{1 - f(r)} + \frac{p_r}{\sqrt{p_r^2 + p_\phi^2/r^2 + m^2}},$$

$$\dot{p}_r = -\frac{\partial E}{\partial r} = -\frac{f'(r)}{2\sqrt{1 - f(r)}}\, p_r + \frac{p_\phi^2}{r^3\sqrt{p_r^2 + p_\phi^2/r^2 + m^2}} - K_r(r - r_c).$$

$$\dot{\phi} = \frac{\partial E}{\partial p_\phi} = \frac{(p_\phi/r^2)}{\sqrt{p_r^2 + p_\phi^2/r^2 + m^2}},$$

$$\dot{p}_\phi = -\frac{\partial E}{\partial \phi} = -K_\phi\, r_{\mathrm{H}}^2(\phi - \phi_c).$$

Numerical Setup

- Mass ratio $m/M \sim 10^{-5}$; choose K_r, K_ϕ, r_c, ϕ_c to keep motion near horizon.
- Integrator: 4th-order Runge–Kutta; fixed step $h \sim 10^{-2}$ (dimensionless units with $G = c = 1$).
- Sample initial conditions: $r \in (3.0, 3.8)$, $p_r \in (-0.5, 0.5)$, $\phi \in (-0.05, 0.05)$; determine p_ϕ from fixed E.

Poincaré Section Construction

- Take section at $\phi = 0$ with $p_\phi > 0$.
- Plot intersections in (r, p_r) for fixed E.
- Closed KAM curves $\Rightarrow$ regular; broken tori/scatter $\Rightarrow$ chaos.

Energy Scan ($r_s = 0.15,\ \rho_s = 0.02$)

- Low E: intact KAM tori (regular motion).
- Intermediate E: distorted tori $\Rightarrow$ onset of chaos.
- High E: widespread scatter $\Rightarrow$ fully chaotic.

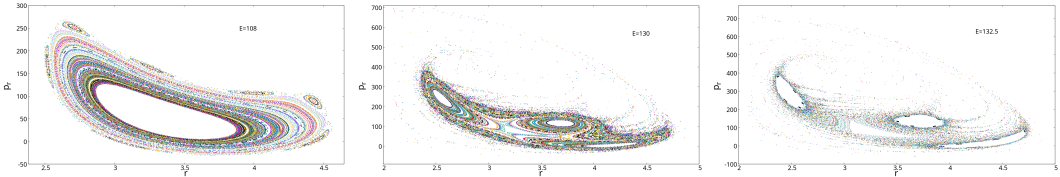

Halo Scan at fixed E and r_s

Fix $r_s = 0.15$, $E = 90$; vary ρ_s.

- Increasing $\rho_s \Rightarrow$ larger effective horizon, stronger nonlinearity.
- Regular $\rightarrow$ onset $\rightarrow$ chaotic as ρ_s grows.

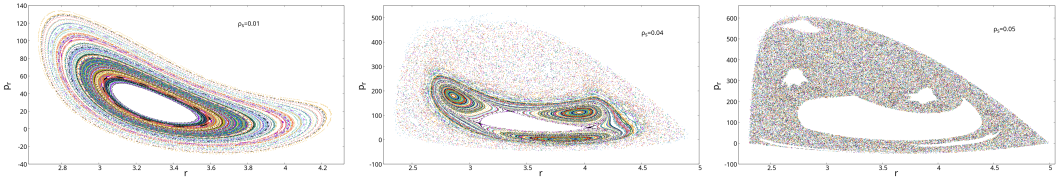

Halo Scan at fixed E and ρ_s

Fix $\rho_s = 0.01$, $E = 115$; vary r_s.

- Larger r_s has similar effect; chaos at higher r_s values.
- Regular $\rightarrow$ onset $\rightarrow$ chaotic as r_s grows.

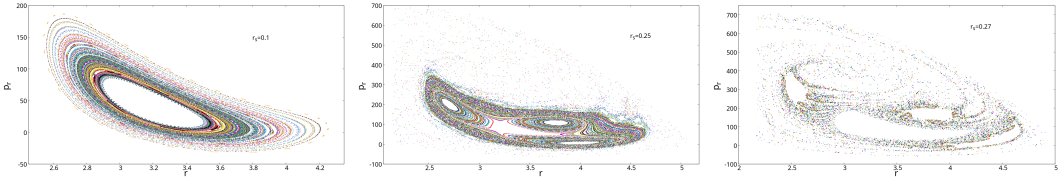

Lyapunov Exponents: Definitions

$$\lambda_{\max} = \lim_{\tau \to \infty} \frac{1}{\tau} \ln \frac{\delta X(\tau)}{\delta X(0)},$$

λ_r : separation measured of two trajectories in phase-space.

- Practical computation: evolve two nearby trajectories; calculate separation in large time limit.

LE Results (Qualitative)

- λ_L increases with E, also with ρ_s and r_s.

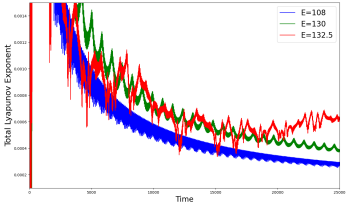

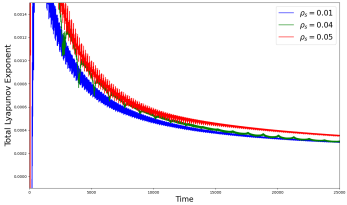

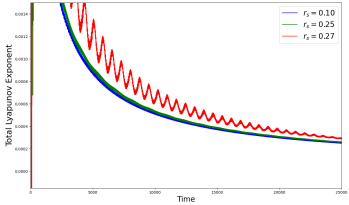

Kludge Strategy

1. Compute geodesic-like trajectory in BH+DM spacetime (PG coords).
2. Map (r, θ, φ) to flat-space spherical, then to Cartesian: $x = r \sin\theta \cos\varphi$, etc.
3. Use flat-space wave-generation (quadrupole) on that trajectory.

Rationale

Trajectory accuracy $\Rightarrow$ essential waveform morphology retained even with simplified radiation model.

From Linearized Gravity to Quadrupole

$$g_{\mu\nu} = \eta_{\mu\nu} + h_{\mu\nu}, \qquad \bar{h}_{\mu\nu} = h_{\mu\nu} - \tfrac{1}{2}\eta_{\mu\nu}h,$$
$$\partial_\alpha \bar{h}^{\mu\alpha} = 0, \qquad \Box \bar{h}^{\mu\nu} = -16\pi T^{\mu\nu}.$$

Retarded solution:

$$\bar{h}^{ij}(t,\mathbf{x}) = 4\int d^3x' \, \frac{T^{ij}(t-|\mathbf{x}-\mathbf{x}'|,\mathbf{x}')}{|\mathbf{x}-\mathbf{x}'|}.$$

Slow-motion limit $\Rightarrow$ quadrupole formula

$$\bar{h}^{ij}(t,\mathbf{x}) = \frac{2}{r}\ddot{I}^{ij}(t-r), \quad I^{ij} = \int d^3x' \, x'^i x'^j T^{00}.$$

Point Particle Source and h_{ij}

For a point mass m at $\mathbf{x}_p(t')$:

$$T^{\mu\nu}(t', \mathbf{x}') = m \frac{dx_p^\mu}{d\tau} \frac{dx_p^\nu}{d\tau} \delta^{(3)}(\mathbf{x}' - \mathbf{x}_p(t')) \frac{d\tau}{dt'},$$
$$\approx m\, u^\mu u^\nu\, \delta^{(3)}(\mathbf{x}' - \mathbf{x}_p(t')).$$

In the slow-motion regime one obtains

$$h_{ij} = \frac{2m}{D_L} \Big(a_i x_j + a_j x_i + 2 v_i v_j \Big),$$

where $\mathbf{x}, \mathbf{v}, \mathbf{a}$ are position, velocity and acceleration along the mapped trajectory, and D_L is the luminosity distance.

Detector Frame and Polarizations

Define detector-aligned basis (X, Y, Z) with inclination ι and pericenter longitude ζ:

$$\begin{aligned}
\mathbf{e}_X &= (\cos\zeta, -\sin\zeta, 0), \\
\mathbf{e}_Y &= (\sin\iota\sin\zeta, -\cos\iota\cos\zeta, -\sin\iota), \\
\mathbf{e}_Z &= (\sin\iota\sin\zeta, -\sin\iota\cos\zeta, \cos\iota).
\end{aligned}$$

Polarizations:

$$\begin{aligned}
h_+ &= \tfrac{1}{2}(e_X^i e_X^j - e_Y^i e_Y^j) h_{ij}, \\
h_\times &= \tfrac{1}{2}(e_X^i e_Y^j + e_Y^i e_X^j) h_{ij}.
\end{aligned}$$

Waveform Morphology

- Regular orbit $\Rightarrow$ quasi-periodic $h_+, h_\times$ with narrow-band spectrum.
- Onset-of-chaos $\Rightarrow$ visible amplitude/phase modulations; sidebands.
- Chaotic $\Rightarrow$ irregular amplitude, broadband features, recurrent bursts.

Waveform structures

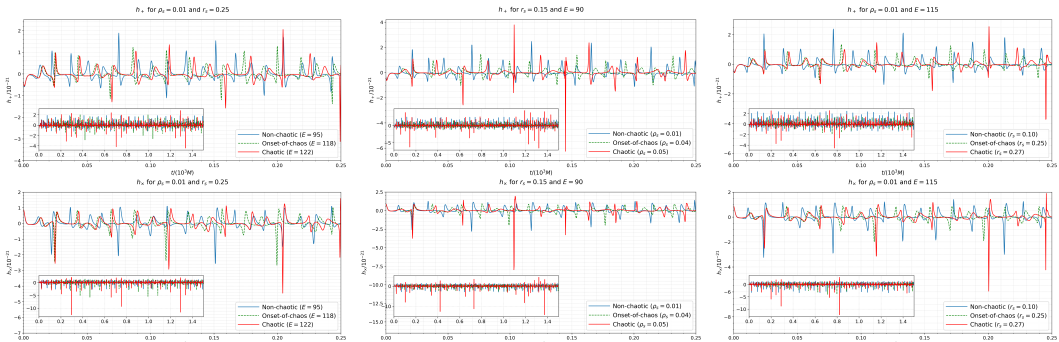

Power Spectral Density

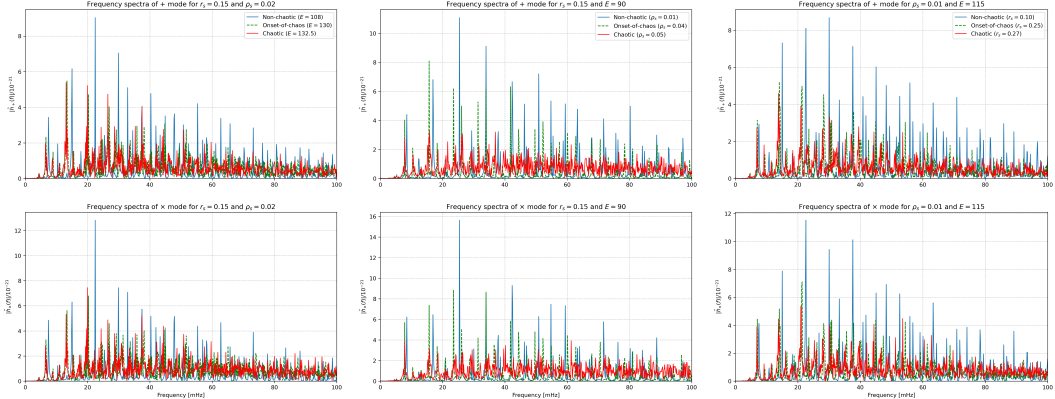

Comparisions of Characteristic strain (for different E)

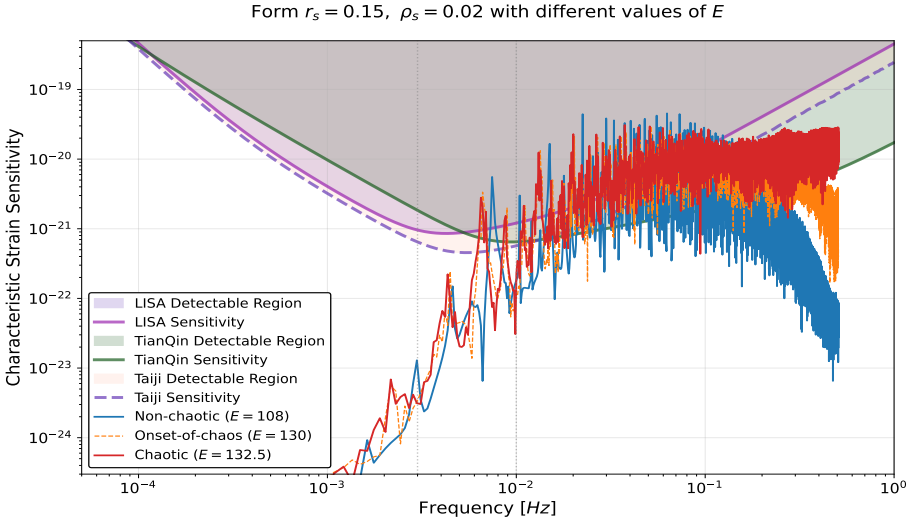

Comparisions of Characteristic strain (for different ρ_s)

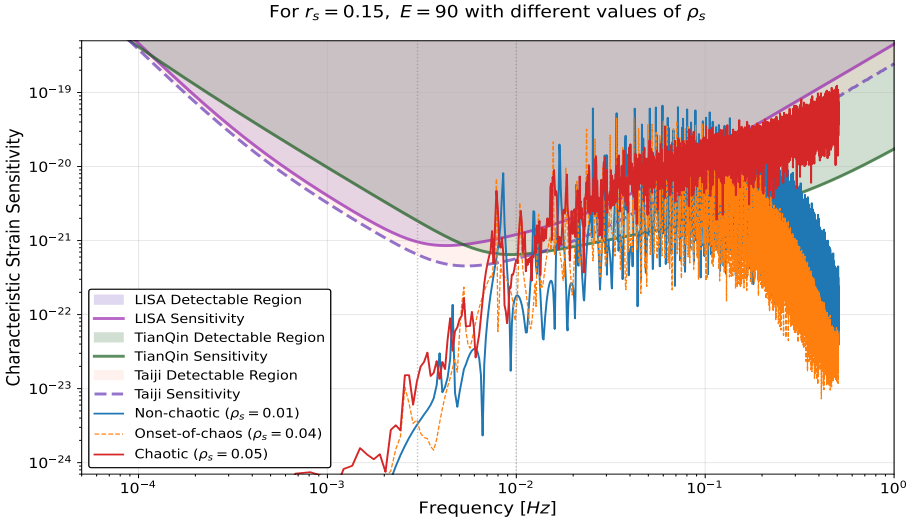

Comparisions of Characteristic strain (for different r_s)

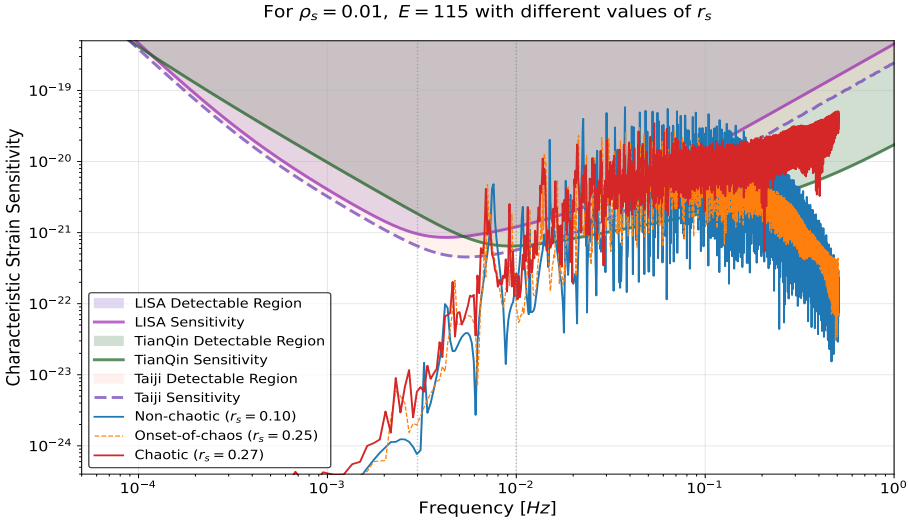

Limitations and Assumptions

- Test-particle limit; neglect self-force and backreaction on halo.
- Leading-order DM effect in $f(r)$; $A(r) = B(r)$ simplification.
- Kludge waveforms: accurate trends, not precision templates.

Conclusions and Outlook

- DM halos can catalyze onset of chaos in near-horizon EMRI dynamics.
- Poincaré maps and Lyapunov exponents quantify transition.
- Kludge GWs show distinctive chaotic imprints (amplitude/phase irregularity, spectral broadening).
- Next: Kerr backgrounds with halo, include radiation reaction/self-force, parameter estimation for chaos.

Thanks for listening!